Analysis of fluctuation conductivity of polycrystalline $Er_{1-x}Pr_xBa_2Cu_3O_{7-\delta}$ superconductors

A.R. Jurelo, R. Menegotto Costa,* A.V.C. de Andrade, P.R. Júnior,
G.K. da Cruz, C.S. Lopes, M. dos Santos, and W.T.B. de Sousa
Departamento de Física, Universidade Estadual de Ponta Grossa,
Av. Gen. Carlos Cavalcanti 4748, 84.030-000, Ponta Grossa, Paraná, Brazil.
(Received on 3 July, 2009)

In this work we report on conductivity fluctuation measurements in polycrystalline samples of the $Er_{1-x}Pr_xBa_2Cu3O_{7-\delta}$ superconductor (x =0.00, 0.05 and 0.10). Samples were prepared by a standard solid-state reaction technique. The results were analyzed in terms of the temperature derivative of the resistivity and of the logarithmic temperature derivative of the conductivity that allowed the identification of power-law divergences of the conductivity. The results show that the transition proceeds in two stages: pairing and coherence transition. Also, our results, from the critical exponent analysis, show a two-peak splitting at pairing transition, indicating possibly a phase separation. On approaching the zero resistance state, our results show a power-law behavior that corresponds to a phase transition from paracoherent to a coherent state of the granular array.

Keywords: High-T_C Superconductor, Erbium, Praseodymium, Critical Phenomena.

1. INTRODUCTION

It is well known that rare earth (RE) substitution for Y in $YBa_2Cu_3O_{7-\delta}$ (Y-123) has little effect on superconductivity, except for Pr, Ce, Tb and Pm [1]. Pr forms a compound that is isostructural with $Y-123$, however it is not a superconductor [2]. On the other hand, Ce and Tb do not form the compound RE-123 [3-5], and Pm is radioactive with a short half life. In particular, $RE_{1-x}Pr_xBa_2Cu_3O_{7-\delta}$ compound has become one of the most studied subjects in the field of high temperature superconductivity. From these studies, it has been observed that increasing Pr substitution in $RE_{1-x}Pr_xBa_2Cu_3O_{7-\delta}$, causes a monotonically decrease in the critical temperature (T_C) [6]. Some mechanisms such as hole localization [7,8], hole filling [9], magnetic pair breaking [10] and percolation [11] have been proposed to explain the degradation of superconductivity. Also, it was observed an ion-size effect in experiments on the $RE_{1-x}Pr_xBa_2Cu_3O_{7-\delta}$ system for RE = Nd, Eu, Gd, Y, Er and Yb, indicating an approximately linear T_C decrease with increasing the RE-site ions radius for a fixed dopant amount x [12]. Yet, some of $REBa_2Cu_3O_{7-\delta}$ compounds (such as for $RE = Nd$, Sm, Gd, Ho and Er) exhibit antiferromagnetic ordering below T_C [13], showing that investigations about the interplay between superconductivity and magnetism can be of particular interest in this system.

Despite the large amount of research on this system, considerable controversy still persists over the mechanisms of T_C suppression by Pr in $RE_{1-x}Pr_xBa_2Cu_3O_{7-\delta}$. Careful studies of the conductivity in the neighborhood of the critical temperature can yield information about the nature of the superconducting state [14-16] as well as on the influence of the granularity at microscopic and mesoscopic levels on the fluctuation regimes [17-19]. In this paper, we report on fluctuations conductivity measurements in polycrystalline samples of the $Er_{1-x}Pr_xBa_2Cu_3O_{7-\delta}$ ($0 \leq x \leq 0.10$) superconductor. The structural characterization of the samples was obtained through Rietveld analysis of the XRD patterns and the results revealed that all samples were nearly single-phase, without

dependence on the Pr concentration. Also, using the temperature derivative of the resistivity, $d\rho/dT$, and the logarithmic temperature derivative of the conductivity, $-d\ln(\Delta\sigma)/dT$, we observed the evolution of the critical regimes as a function of praseodymium concentration.

2. EXPERIMENTAL DETAILS

Polycrystalline samples of $Er_{1-x}Pr_xBa_2Cu_3O_{7-\delta}$ (x =0.00, 0.05 and 0.10) were prepared by solid-state reaction technique, using Er_2O_3, Pr_6O_{11}, $BaCO_3$, and CuO. Appropriate amounts were mixed and calcinated in air at 850, 880 and 920^0C for 24 hours, and then slowly cooled through 700^0C. Finally, the samples were heated in flowing oxygen at $400\ ^0C$ for 48 hours. The resistivity measurements were performed with a low-frequency-low-current AC technique that employs a lock-in amplifier as a null detector. The measurements current density was up to 600 mA/cm^2. To provide electrical contact to the sample, four stripes of silver paste were painted onto the surface. The silver paint was fixed to the sample by heating it in flowing O_2 for 4 h at 400 ^0C. Then, copper wires were attached to the samples with silver paste, resulting in contact resistance of less than 1 ohm. Temperature was measured with a Pt sensor, allowing a resolution better than 1 mK, and the resistivity measurements were performed at a 3 K/h rate or lower.

X-ray powder diffraction patterns were collected from 5^0 to 100^0 in the 2θ range with 0.02^0 step and 4 s counting time. Rietveld refinements of crystal structures were performed using the GSAS and EXPGUI software [20,21]. The X-ray powder diffraction patterns of $Er_{1-x}Pr_xBa_2Cu_3O_{7-\delta}$ for $x = 0.00$, $x = 0.05$ and $x = 0.10$ are displayed in Fig. 1. The X-ray pattern almost completely matches the orthorhombic $Er-123$ structure (compared with JCPDS files), and belongs to the $ErBa_2Cu_3O_{7-\delta}$ orthorhombic unit cell with symmetry $Pmmm$. Also, all samples were found to be nearly single-phase, and show no dependence on the Pr concentration or the presence of trace impurities of $BaCuO_2$, $PrBaO_3$ and CuO. The presence of $BaCuO_2$ phase is a result of substitution of Pr at Ba site, while the observation of small quantities of the $BaCuO_2$ and $PrBaO_3$ impurity phases is a

———————
*Electronic address: rmcosta@uepg.br

TABLE I: Unit cell parameters, atomic parameters, and agreement factors for $Er_{1-x}Pr_xBa_2Cu_3O_{7-\delta}$; $x = 0.00$, $x = 0.05$ and $x = 0.10$; obtained through Rietveld refinements at room temperature.

	$ErBa_2Cu_3O_{7-\delta}$ ($x = 0.00$)	$Er_{0.95}Pr_{0.05}Ba_2Cu_3O_{7-\delta}$ ($x = 0.05$)	$Er_{0.95}Pr_{0.05}Ba_2Cu_3O_{7-\delta}$ ($x = 0.10$)
a(Å)	3.8236 (1)	3.8183 (1)	3.8165 (1)
b (Å)	3.8792 (1)	3.8855 (1)	3.8839 (2)
c (Å)	11.6778 (2)	11.6739 (2)	11.6730 (2)
V (Å^3)	173.213 (8)	173.197 (8)	173.03 (1)
R$_p$ (%)	8.91	9.59	11.60
R$_{wp}$ (%)	11.51	12.48	15.04
χ^2	1.431	1.766	1.255
R$_e$ (%)	9.69	9.39	11.98

characteristic of Pr-rich samples [22,23].

The unit cell parameters, atomic parameters, and agreement factors for $Er_{1-x}Pr_xBa_2Cu_3O_{7-\delta}$ ($x = 0.00$, $x = 0.05$ and $x = 0.10$) obtained through Rietveld refinements at room temperature are summarized in Table I. The value of the lattice parameter a decreases from 3.8236 (1) Å for $x = 0.00$ to 3.8165 (1) Å for $x = 0.10$ while c also decreases from 11.6778 (2) Å for $x = 0.00$ to 11.6730 (2) Å for $x = 0.10$. Meanwhile, b increases from 3.8792 (1) Å to 3.8839 (2) Å . Also, the volume decreases from 173.213 (8) Å^3 for $x = 0.00$ to 173.03 (1) Å^3 for $x = 0.10$. In a general manner, the lattice parameters and volume derived from least squares refinement are in agreement with published results obtained in others studies [24,25]. From Table I we can observe that R_P ($R-$pattern), R_{wp} ($R-$w eighted pattern), R_e ($R-$ expected) and $\chi^2 = \sqrt{R_{wp}/R_e}$ (goodness-of-fit) systematically increase with increasing x. However, as the R_i factors are small, the results are reliable [26,27].

3. RESULTS AND DISCUSSION

It is well-known that sintered samples of high temperature superconductors show a pronounced granular character that plays an important role in their resistive transition. As the temperature decreases from the normal state, it is first observed a pairing transition and then a coherence transition. At the pairing transition, the superconductivity is stabilized in some small and homogeneous regions of the sample at a temperature which virtually coincides with the critical temperature of the bulk, T_C. These superconducting grains may not necessarily be coincident with the crystallographic grains. At a lower temperature, T_{CO}, the superconductivity is established among the grains. This is the coherence transition, a long-range superconducting state that is achieved through a percolation-like process which controls the activation of weak links between grains. This behavior is very common in polycrystalline samples and it is associated with disorder at mesoscopic level.

In Fig. 2 we show the superconducting transition for three $Er_{1-x}Pr_xBa_2Cu_3O_{7-\delta}$ samples: $x = 0.00$ (open circle), $x = 0.05$ (open square) and $x = 0.10$ (closed circle).

The measurements were performed with current density of $J = 60\ mA/cm^2$ and the room-temperature resistivities were $\rho(300\ K) = 3.3\ m\,\Omega\ cm$ ($x = 0.00$), 6.0 m Ω cm ($x = 0.05$) and 2.4 $m\,\Omega\ cm$ ($x = 0.10$). The presented data are normalized to unity at 95 K. The results (not shown) also indicate that our samples present a metallic-like behavior at high temperatures. The panels (a) and (c) show the resistivity versus temperature plots whereas panels (b) and (d) show the plot of $d\rho/dT$ versus temperature in the corresponding temperature range. The plots of $d\rho/dT$ versus temperature, shown in panels (b) and (d), present two maxima denoted by T_{P1} and T_{P2}. These two peaks are associated with a splitting of the pairing transition. The maxima T_{P1} and T_{P2} correspond approximately to the pairing critical temperatures T_{C1} and T_{C2}, respectively. T_{P1} is approximately 91.8 K ($x = 0.00$), 93.0 K ($x = 0.05$) and 88.2 K ($x = 0.10$) and T_{P2} is about 91.2 K ($x = 0.05$) and 85.6 K ($x = 0.10$). These results indicate that the superconducting pairing transition occurs in two steps of about 1.8 K apart ($x = 0.05$ sample) and with about 4 K ($x = 0.10$ sample). It is interesting to note that for low concentration of praseodymium ($x = 0.05$), the value of T_{P1} is higher than that for the pure system. This effect was also observed for other doped samples [28]. From panels (c) and (d) we can observe that 10 % Pr substitution in the Er sites causes a strong depression of the superconducting transition temperature and a significant enlargement of the width of the resistive transition (10 % to 90 % of the transition) of approximately 2.0 K ($x = 0.00$) to 6 K ($x = 0.10$). For the $x = 0.10$ sample, the whole transition broadens.

3.1. Method of Analysis

We study the effect of thermal fluctuations to the conductivity by using a Kouvel-Fischer-type method [29]. It is assumed that the fluctuation conductivity $\Delta\sigma$ diverges as a power-law given by

$$\Delta\sigma = A\varepsilon^{-\lambda}, \qquad (1)$$

where $\Delta\sigma = \sigma - \sigma_R$, A is the critical amplitude, $\varepsilon = (T - T_C)/T_C$ is the reduced temperature and λ is the critical exponent. From the resistivity measurements, we calculate
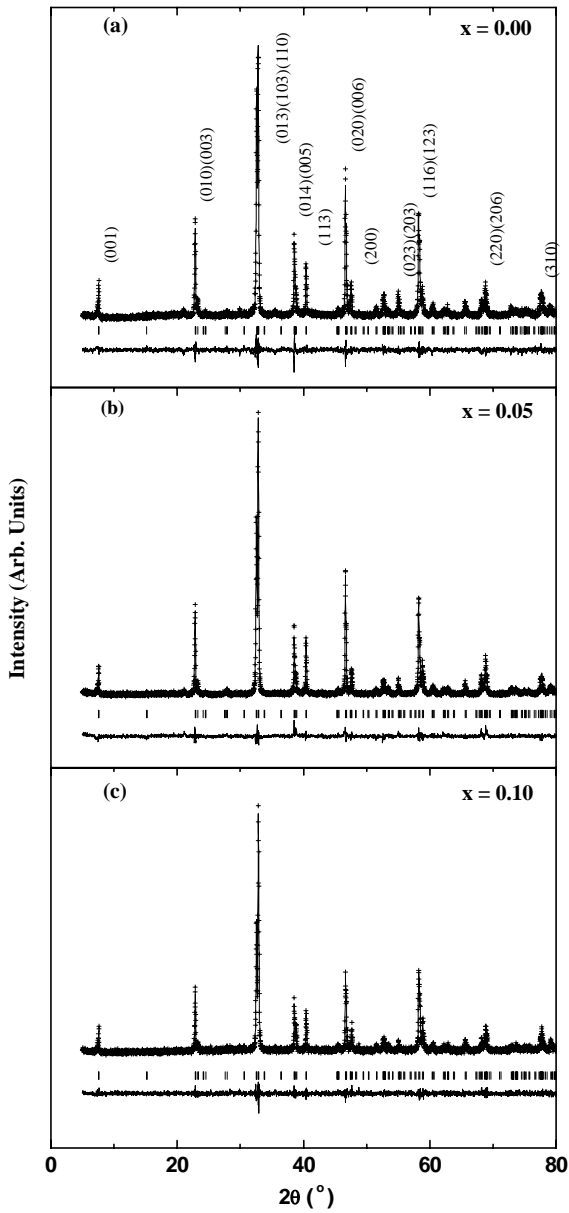
FIG. 1: Room temperature XRD patterns of polycrystalline samples of $Er_{1-x}Pr_xBa_2Cu_3O_{7-\delta}$: (a) $x = 0.00$, (b) $x = 0.05$ and (c) $x = 0.10$. The lower curve is the difference between the observed and the calculated intensities.

the conductivity $\sigma = 1/\rho$. σ_R, the regular conductivity, is obtained by linear extrapolation of the resistivity data in the range from $2T_C$ to room temperature.

To obtain the values for λ e T_C, we determine numerically the logarithmic derivative of $\Delta\sigma$ from experimental data and define

$$\chi_\sigma = -\frac{d}{dT}\ln\Delta\sigma. \qquad (2)$$

Combining eqs. (1) and (2) we obtain

$$\frac{1}{\chi_\sigma} = \frac{1}{\lambda}(T - T_C). \qquad (3)$$
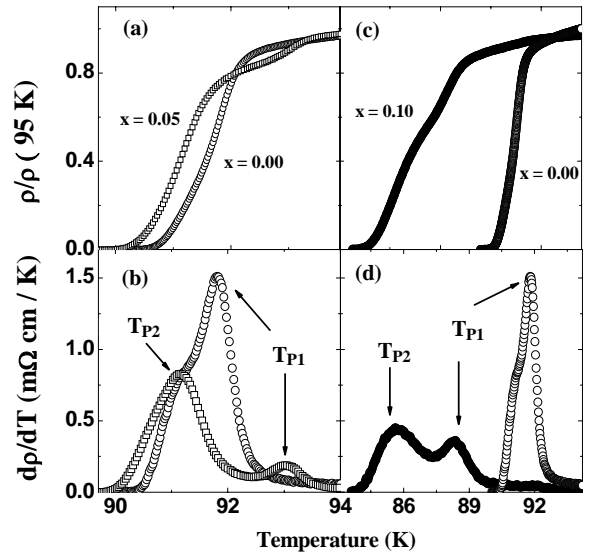

FIG. 2: The panels (a) and (c) show the resistivity versus temperature plot while the panels (b) and (d) show the temperature derivative of the resistivity versus temperature, around of the critical temperature, for three $Er_{1-x}Pr_xBa_2Cu_3O_{7-\delta}$ samples: $x = 0.00$ (open circle), $x = 0.05$ (open square) and $x = 0.10$ (closed circle). The temperature T_P corresponds approximately to the intragrain pairing transition. The current density was $60\ mA/cm^2$.
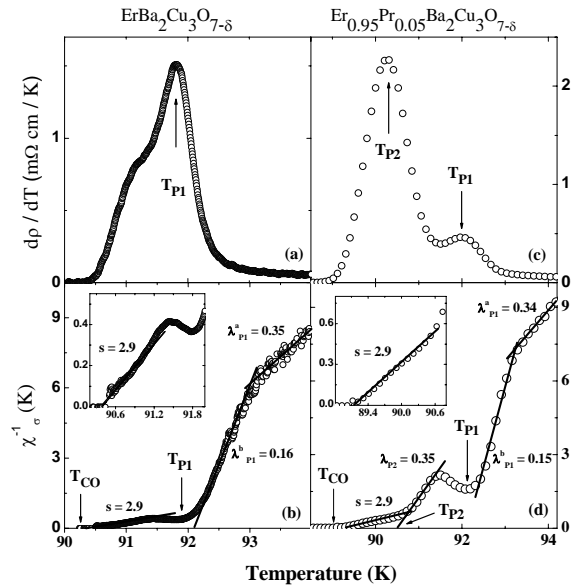

FIG. 3: Panels (a) and (b) show representative results of the resistive transition ($J = 60\ mA/cm^2$) for a $ErBa_2Cu_3O_{7-\delta}$ sample and panels (c) and (d) for a $Er_{0.95}Pr_{0.05}Ba_2Cu_3O_{7-\delta}$ sample. Panels (a) and (c) show $d\rho/dT$ versus temperature and panels (b) and (d) the inverse of the logarithmic derivative of the conductivity (χ_σ^{-1}) as a function of T. The straight lines correspond to fits to Eq. (3) and the respective exponents are quoted. The inserts show an expanded view of the asymptotic regime of the coherence transition.
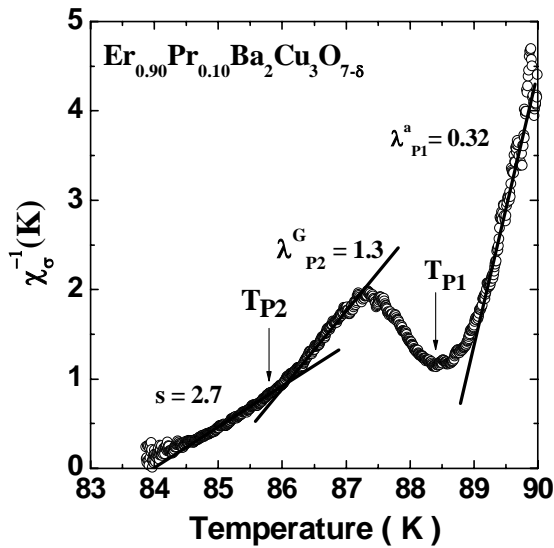
FIG. 4: The inverse of the logarithmic derivative of the conductivity χ_σ^{-1} as a function of T obtained for a sample of $Er_{0.90}Pr_{0.10}Ba_2Cu_3O_{7-\delta}$ ($J = 60\ mA/cm^2$).

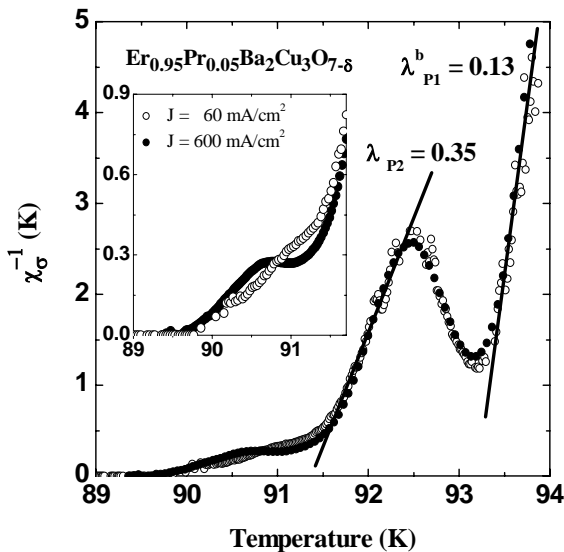FIG. 5: The inverse of the logarithmic derivative of the conductivity χ_σ^{-1} as a function of T obtained for a sample of $Er_{0.95}Pr_{0.05}Ba_2Cu_3O_7$ with $J = 60\ mA/cm^2$ and $J = 600\ mA/cm^2$. The respective exponents are quoted. The insert shows an expanded view close to $R = 0$ state.

Then, it is possible to determine simultaneously T_C and λ by plotting χ_σ^{-1} versus T [14]. Performing averages over several measurements, we obtained the mean values of the critical exponents.

3.2. Critical Fluctuation Regimes

In Fig. 3 we compare the resistive transitions of $ErBa_2Cu_3O_{7-\delta}$ ($x = 0.00$) and $Er_{0.95}Pr_{0.05}Ba_2Cu_3O_{7-\delta}$ ($x = 0.05$) measured with current density of $J = 60\ mA/cm^2$. In panels (a) and (c), $d\rho/dT\ x\ T$ is plotted. In panels (b) and (d), the transition is shown as $\chi_\sigma^{-1}\ x\ T$ in the corresponding temperature interval. The figure allows the identification of the asymptotic regime of the coherence critical region (between T_{CO} and T_{P1} for $x =0.00$ sample and between T_{CO} and T_{P2} for $x =0.05$ sample) and of the pairing critical region (above T_{P1} for $x =0.00$ sample and above T_{P2} for $x =0.05$ sample). The pairing critical region has an internal structure [16], and two power-law regimes are observed in sequence when T approaches T_{C1} from above corresponding to $\lambda_{P1}^a \approx 0.34$ and $\lambda_{P1}^b \approx 0.15$.

From panel 3(b) we can observe, above T_{P1}, a full dynamic regime dominated by genuine critical flucutations labeled by the exponent $\lambda_{P1}^a = 0.35 \pm 0.03$. The value of the exponent λ_{P1}^a is consistent with the predictions for the 3D-XY universality class [14]. Still closer to T_{C1}, it is observed a fluctuation regime beyond 3D-XY with an exponent $\lambda_{P1}^b = 0.16 \pm 0.03$. This scaling might represent a crossover to an ultimate weakly first-order character of the normal superconducting transition of high temperature cuprates [16]. This critical regime was previously observed in polycrystalline and single-crystal samples [16,30]. Yet, from panel 3(b), we can observe near the zero resistance state (T_{CO}) that the fluctuation conductivity can be described by an another power law, given by the equation $\Delta\sigma \propto (T - T_{CO})^{-s}$, with exponent $s = 2.9 \pm 0.3$. The insert shows an expanded view of the asymptotic regime of the coherence critical regime. This regime is interpreted as being intrinsically related to superconducting granularity at mesoscopic level. When the disorder at mesoscopic level dominates, the fluctuation conductivity near the zero-resistance state must diverge with an exponent quite large ($s \cong 3.0$) [31]. The value $s \sim 2.9$ observed for this sample is according to the expected value for critical conductivity fluctuations in artificially prepared granular arrays, $s \cong 3$ [32]. The same exponent was also observed to characterize the resistive paracoherence-coherence transition of Y-123 ceramics [14,33].

In panel 3(d), it is observed in sequence, again, two power-law regimes when T approaches T_{C1} from above corresponding to $\lambda_{P1}^a = 0.34 \pm 0.03$ and $\lambda_{P1}^b = 0.15 \pm 0.02$. The value $\lambda_{P1}^a = 0.34$ reveals the effects of genuine fluctuations which belong to the 3D-XY univesarlity class. In the immediate vicinity above T_{P1} we identify a genuinely critical fluctuation regime described by the exponent $\lambda_{P1}^b = 0.15$, which is precursor of a weakly first-order transition [16]. Another genuinely critical regime represented by the exponent $\lambda_{P2} = 0.35 \pm 0.03$ is also visible below T_{P1}, in the immediate vicinity above T_{P2}. This regime, that was not observed in the $x = 0.00$ sample, is in agreement with the predictions of the full dynamic 3D-XY model [14]. The splitting of the pairing transition, verified by observation of critical regimes λ_{P1}^a and λ_{P1}^b (above T_{P1}) and λ_{P2} (below T_{P1}), could be produced by the presence of two superconducting phases with different temperature transition induced by microscopic granularity. The results displayed in Fig. 2(b) suggest that Pr doping in-

duces a superconducting phase with higher critical temperature ($\sim 93.1\ K$). A genuine critical fluctuation regime in the temperature range between T_{P2} and T_{P1} was first observed by Barros *et al.* in $Y_{1-x}Pr_xBa_2Cu_3O_{7-\delta}$ single crystals and polycrystalline samples [19,30], and it was associated with a peculiar phase separation related with oxygen doping. Panel 3(d) also shows that, between T_{P2} and T_{C0}, the variation of χ_σ^{-1} as a function of temperature is well described by a power law regime with corresponding exponent $s = 2.9 \pm 0.3$. The insert shows an expanded view of the paracoherence temperature region. This value is the same observed in the pure system and is interpreted as an indication of a paracoherent-coherent transition of the granular array [14,30].

Fig. 4 displays representative plots of χ_σ^{-1} x T for the $Er_{0.90}Pr_{0.10}Ba_2Cu_3O_{7-\delta}$ ($x = 0.10$) sample for $J = 60$ mA/cm^2. Above T_{P1}, the results show the occurrence of a genuine critical regime, with exponent $\lambda_{P1}^a = 0.32 \pm 0.01$ that is consistent with the predictions for the $3D - XY$ universality class. It is important to point out that, in this case, a scaling beyond $3D - XY$ precursor of a weakly first-order transition [16] was not observed, as noticed for the $Y_{0.95}Pr_{0.05}Ba_2Cu_3O_{7-\delta}$ and pure samples. Between T_{P2} and T_{P1} we can clearly observe another fluctuation regime with exponent $\lambda_{P2}^G = 1.3 \pm 0.2$. This exponent does not correspond to an integer dimensionality. In this case we suppose that the flucutations develop in a space having fractal topology. According to Char and Kapitulnik [34], the conductivity exponent should be written as $\lambda = 2 - \frac{\tilde{d}}{2}$ where $\tilde{d}$ is the fractal dimension of the flucutation network. Our exponent $\lambda_{P2}^G \approx 1.3$ is consistent with $\tilde{d} \approx \frac{4}{3}$, which is the weel-known fractal dimensionality of the percolation network [35] that corresponds to a crossover regime between 1D and 2D geometry. A similar exponent was also observed in Bi based cuprates [14, 36]. We expected the presence of the $3D - XY$ scaling closer to T_{P2} in the $x = 0.10$ sample, as observed for the $x = 0.00$ and $x = 0.05$ samples. The disappearance of this regime is cleary related with the increase in Pr doping. The observation of the Gaussian regime is related with its robustness against the Pr doping. Again, in approaching the zero resistance state, our results show a power-law behavior with critical exponent $s = 2.7 \pm 0.1$ that corresponds to a phase transition from a paracoherent to a coherent state of the granular array [31]. These results indicate that an increasing Pr concentration destroys the pairing critical regimes. On the other hand, 10% of Pr substitution does not affect the coherent transition.

Fig. 5 compares representative plots of χ_σ^{-1} x T for the $x = 0.05$ sample for two different currents density, $J = 60$ mA/cm^2 and $J = 600\ mA/cm^2$. We can observe that the regimes λ_{P1}^b and λ_{P2} are stable against J within the studied range. This behavior is consistent with the interpretation that the observed λ_{P2} regime is related with a pairing (intragrain) transition. Below T_{P2}, and down to the zero-resistance state, the resistivity is current dependent. The figure shows that

the higher current intensity shifts T_{CO} to lower temperatures. Thus, the enlargement of the resistive transition induced by current in our samples is an effect directly related to granularity. Indeed, the self-field is expected to enhance the granular character of the samples by weakening the junctions between grains. The effect of increasing current for the $x = 0.10$ sample (not shown) is similar to that observed for the $x = 0.05$ sample.

The comparison of the results obtained in the pure and doped systems shows that the Pr doping (until 10 %) alters significantly the critical behavior of the $Er_{1-x}Pr_xBa_2Cu_3O_{7-\delta}$ compound above T_{P2}. Two possible Pr doping effects can be inferred from our experiments and analysis. The first one is a phase separation, showed in Figs. 3, 4 and 5, and that is indicated by the presence of two genuinely critical regimes above T_{P2}. These critical regimes are not affected by the studied currents. The second effect is the weakness of the superconductivity, which can be observed by the suppression of the pairing critical regimes. The regime beyond $3D - XY$ ($\lambda \approx 0.13$), observed above T_{P1} for $x = 0.00$ and $x = 0.05$ samples, was not observed for the $x = 0.10$ sample. At the same time, the critical regime $3D - XY$ ($\lambda \approx 0.33$) observed between T_{P1} and T_{P2} for the $x = 0.05$ sample, was also suppressed in the $x = 0.10$ sample. On the other hand, below T_{P2}, in the paracoherent regime, it was not observed any influence of the Pr doping on the critical exponents. These results indicate that Pr doping induces structural disorder at a microscopic level in the studied system.

4. CONCLUSIONS

In conclusion, our conductivity experiments on granular $Er_{1-x}Pr_xBa_2Cu_3O_{7-\delta}$ ($0 \leq x \leq 0.10$) samples show that the superconducting transition proceeds in two stages: pairing and coherence transition. From the temperature derivative and power-law divergences of the conductivity, our results show a two-peak splitting at pairing transition, indicating possibly a peculiar phase separation associated with Pr doping. Another Pr doping effect is the weakness of the superconductivity, which can be observed through the suppression of genuine critical regimes. On approaching the zero resistance state, our results show a power-law behavior that corresponds to a phase transition from paracoherent to a coherent state of the granular array with exponents that are doping independent.

[1] H. B. Radousky, J. Mater. Res. **7**, 1917 (1992).

[2] L. Soderholm, K. Zhang, D. G. Hinks, M. A. Beno, J. D. Jorgenson, C. U. Segre and I. K. Schuller, Nature **328**, 604 (1987).

[3] S. Ohshima and T. Wakiyama, Jpn. J. Appl. Phys. **26**, L815 (1987).

[4] S. Tsurumi, M. Hikita, T. Iwata, K. Semba and S. Kurithara, Jpn. J. Appl. Phys. **26**, L856 (1987).

[5] T. Tamegai, A. Watanabe, I. Oguro and Y. Iye, Jpn. J. Appl. Phys. **26**, L1304 (1987).

[6] Y. Dalichaouch, M. S. Torikachvili, E. A. Early, B. W. Lee, C. L. Seaman, K. N. Yang, H. Zhou and M. B. Maple, Solid State Commun. **65**, 1001 (1988).

[7] R. Fehrenbacher and T. M. Rice, Phys. Rev. Lett. **70**, 3471 (1993).

[8] A. I. Liechtenstein and I. I. Mazin, Phys. Rev. Lett. **74**, 1000 (1995).

[9] J. L. Peng, P. Klavins, R. N. Shelton, H. B. Radousky, P. A. Hahn and L. Bernardez, Phys. Rev. B **40**, 4517 (1989).

[10] J. J. Neumeier, T. Bjornholm, M. B. Maple and I. K. Schuller, Phys. Rev. Lett. **63**, 2516 (1989).

[11] C. Infante, M. K. El Mously, R. Dayal, M. Husain, S. A. Siddiqi and P. Ganguly, Physica C **167**, 640 (1990).

[12] Y. Xu and W. Guan, Phys. Rev. B **45**, 3176 (1992).

[13] B. W. Lee, J. M. Ferreira, S. Ghamaty, K. N. Yang and M. B. Maple, in *Oxygen Disorder Effects in High-T_C Superconductors,* ed. J. L. Moran-Lopez and Ivan K. Schuller, Plenum Press, New York and London, 1990.

[14] P. Pureur, R. M. Costa, P. Rodrigues Jr., J. Schaf and J. V. Kunzler, Phys. Rev. B **47**, 11420 (1993).

[15] R. M. Costa, P. Pureur, L. Ghivelder, J. A. Camp and I. Rasines, Phys. Rev. B **56**, 10836 (1997).

[16] R. M. Costa, P. Pureur, M. Gusmo, S. Senoussi and K. Behnia, Solid State Commun. **113**, 23 (2000).

[17] A. R. Jurelo, J. V. Kunzler, J. Schaf, P. Pureur and J. Rosenblatt, Phys. Rev. B **56**, 14815 (1997).

[18] J. Roa-Rojas, R. M. Costa, P. Pureur and P. Prieto, Phys. Rev. B **61**, 12457 (2000).

[19] F. M. Barros, F. W. Fabris, P. Pureur, J. Schaf, V. N. Vieira, A. R. Jurelo and M. P. Canto, Phys. Rev. B **73**, 94515 (2006).

[20] A. C. Larson and R. B. Von Dreele, *General Structure Analysis System (GSAS)*, Los Alamos National Laboratory Report LAUR 86-748 (1994).

[21] B. H. Toby, J. Appl. Cryst. **34**, 210 (2001).

[22] M. Kariminezhad and M. Akhavan, Physica C **423**, 163 (2005).

[23] Z. Yamani and M. Akhavan, Solid State Commun. **107**, 197 (1998).

[24] J. R. O'Brien and H. Oesterreicher, Journal of Alloy and Compounds **267**, 70 (1998).

[25] S. A. Antony, K. S. Nagaraja, S. Sahasranaman and O. M. Sreedhran, Physica C **323**, 115 (1999).

[26] M. R. Mohammadizadeh, H. Khosroabadi and M. Akhavan, Physica B **321**, 301 (2002).

[27] H. M. Luo, B. N. Lin, Y. H. Lin, H. C. Chiang, Y. Y. Hsu, T. I. Hsu, T. J. Lee, H. C. Ku, C. H. Lin, H. –C. I. Kao, J. B. Shi, J. C. Ho, C. H. Chang, S. R. Hwang and W. –H. Li, Phys. Rev. B **61**, 14825 (2000).

[28] A. R. Jurelo, P. Rodrigues Jr. and R. M. Costa, Modern Physics Letters B **23**, 1367 (2009). Accepted paper "Fluctuation conductivity and phase separation in polycrystalline $Y_{1-x}Ce_xBa_2Cu_3O_{7-\delta}$" in the J Supercond Nov Magn.

[29] J. S. Kouvel and M. E. Fischer, Phys. Rev. **136**, A1616 (1964).

[30] A. R. Jurelo, P. Rodrigues Jr. and J. Flemming, Physica C **349**, 75 (2001).

[31] A. R. Jurelo, I. A. Castillo, J. Roa-Rojas, L. M. Ferreira, L. Ghivelder, P. Pureur and P. Rodrigues Jr., Physica C **311**, 133 (1999).

[32] J. Rosenblatt, in *Percolation, Localization and Superconductivity,* Vol. 109 *of NATO Advanced Study Institute, Series B-Physics*, edited by A. M. Goldman and S. A. Wolf (Plenum, New York, 1984), P. 431.

[33] P. Peyral, C. Lebeau, J. Rosenblatt, A. Raboutou, C. Perrin, O. Pena and M. Sergent, J. Less-Common Met. **151**, 49 (1989).

[34] K. Char and A. Kapitulnik, Z. Phys. B **72**, 253 (1988).

[35] S. Alexander and R. Orbach, J. Phys. Lett (Paris) **43**, L625 (1982).

[36] P. Pureur, R. M. Costa, P. Rodrigues Jr., J. V. Kunzler, J. Schaf, L. Ghivelder, J. A. Camp and I. Rasines, Physica C **235-240**, 1939 (1994).